



Characterization of atmospheric emission sources in lichen from metal and organic contaminant patterns

Aude Ratier^{1,2} · Julien Dron¹ · Gautier Revenko¹ · Annabelle Austruy¹ · Charles-Enzo Dauphin¹ · Florence Chaspoul³ · Emmanuel Wafo⁴

Received: 7 November 2017 / Accepted: 26 December 2017
© Springer-Verlag GmbH Germany, part of Springer Nature 2018

Abstract

Lichen samples from contrasted environments, influenced by various anthropic activities, were investigated focusing on the contaminant signatures according to the atmospheric exposure typologies. Most of the contaminant concentrations measured in the 27 lichen samples, collected around the industrial harbor of Fos-sur-Mer (France), were moderate in rural and urban environments, and reached extreme levels in industrial areas and neighboring cities (Al up to 6567 mg kg⁻¹, Fe 42,398 mg kg⁻¹, or ΣPAH 1417 μg kg⁻¹ for example). At the same time, a strong heterogeneity was noticed in industrial samples while urban and rural ones were relatively homogeneous. Several metals could be associated to steel industry (Fe, Mn, Cd), road traffic, and agriculture (Sb, Cu, Sn), or to a distinct chemical installation (Mo). As well, PCDFs dominated in industrial samples while PCDDs prevailed in urban areas. The particularities observed supported the purpose of this work and discriminated the contributions of various atmospheric pollution emission sources in lichen samples. A statistical approach based on principal component analysis (PCA) was applied and resolved these potential singularities into specific component factors. Even if a certain degree of mixing of the factors is pointed out, relevant relationships were observed with several atmospheric emission sources. By this methodology, the contribution of industrial emissions to the atmospheric metal, PAH, PCB, and PCDD/F levels was roughly estimated to be 60.2%, before biomass burning (10.2%) and road traffic (3.8%). These results demonstrate that lichen biomonitoring offers an encouraging perspective of spatially resolved source apportionment studies.

Keywords Lichen bioaccumulation · Metal · PAH · PCB · PCDD/F · Contaminant profiles · Source apportionment · Industrial emission sources

Responsible editor: Constantini Samara

Electronic supplementary material The online version of this article (<https://doi.org/10.1007/s11356-017-1173-x>) contains supplementary material, which is available to authorized users.

✉ Julien Dron
julien.dron@institut-ecocitoyen.fr

¹ Institut Ecocitoyen pour la Connaissance des Pollutions, 13270 Fos-sur-Mer, France

² Irstea, UR MALY, Centre de Lyon-Villeurbanne, 5 avenue de la Doua—CS20244, 69625 Villeurbanne Cedex, France

³ Laboratoire de Chimie Physique et Prévention des risques et Nuisances Technologiques, IMBE, UMR 7263 CNRS/IRD/Aix Marseille Université/Avignon Université, Marseille, France

⁴ Laboratoire de Chimie Analytique, IMBE UMR 7263 CNRS/IRD237—UMR 1062 INSERM/INRA1260/NORT: Nutrition, Obésité et Risques Thrombotique—UMR 910 Génétique, Aix-Marseille Université/Université d'Avignon, Marseille, France

Introduction

The adverse effects of atmospheric metallic and organic contaminants, such as polycyclic aromatic hydrocarbons (PAHs), polychlorinated biphenyls (PCBs), and dibenzodioxins and furans (PCDD/F)s, on the environment and human health are long since considered (Stockholm Convention 2001; IARC 2013; EEA 2016). In contrast to instrumented techniques, atmospheric biomonitoring allows the simultaneous sampling of numerous locations for the determination of a wide panel of contaminants integrating a long time range.

Among the various air bioindication methods, biomonitoring with lichens has demonstrated a great potential in evaluating the exposure to atmospheric pollution (Nimis et al. 2002; Augusto et al. 2013), potentially offering capabilities to discriminate pollution sources from their contaminant accumulation pattern. These symbiotic organisms, lacking protective cuticle and root system, are essentially dependent of

atmospheric inputs. Their biological activity is permanent throughout the year, allowing bioaccumulation studies during winter as well as other seasons. A number of works were concerned with metal elements, demonstrating the incidence of human activities on their bioaccumulation in lichens (Brunialti and Frati 2007; Occelli et al. 2016; Boonpeng et al. 2017). A more limited number of studies carried out for PAH determination in lichens also depicted the anthropic impact, either from road traffic, industry, or biomass burning (Augusto et al. 2013; Kodnik et al. 2015; Van der Wat and Forbes 2015). Literature also reports some PCDD/F measurements in lichens (Augusto et al. 2015; Protano et al. 2015), and Augusto et al. (2016) recently qualified a particular industrial source from other influences by examining their PCDD/F congener profiles.

Determining the different sources involved into the ambient air contaminant concentrations is a key element when planning to reduce the exposure to atmospheric pollutants. Also, rational information about emission source contributions is particularly valuable to local stakeholders willing to optimize their efforts regarding health and environmental threats. Generally, atmospheric source apportionment methods involve active sampling or on-line measurements. Those are thus limited to one or a very few locations but gather short time-resolved data which can be correlated to meteorological measurements (Viana et al. 2008). In lichen samples, the evaluation of pollution sources is limited to a very few recent studies through the analysis of contaminant profiles, either metals (Hissler et al. 2008; Agnan et al. 2015; Boamponsem et al. 2017; Boonpeng et al. 2017), PAHs (Augusto et al. 2009) or PCDD/Fs (Augusto et al. 2016), but never all together. Nevertheless, using lichen biomonitoring to achieve a spatial distribution of identified contributions of emission sources to atmospheric pollution would be very complementary to instrumental time-resolved methods and would become particularly helpful to stakeholders.

In the very industrialized and contrasted region of Fos-sur-Mer and Berre Lagoon (Provence, France), petrochemical and steel industry activities are major atmospheric emission sources among other industries, biomass burning, road traffic, and ship emissions. *Xanthoria parietina* sampling was held in 27 sites in January 2015 for the determination of metals, PAHs, PCDD/Fs, and PCBs. The aim of the study was primarily to identify specific profiles that could be associated to known emission sources. The hierarchical clustering and principal component analysis (PCA) multivariate analysis methods were performed with the gathered data to identify the contaminants that could be related to emission sources and eventually draw some particular patterns. The PCA was preferred here as a first step to identify specific and consistent factors in locations potentially influenced by numerous and contrasted emission sources (Christensen et al. 2018). Consequently, it focuses in a first place towards contaminant

profiles combining metals and organics in all samples and aims to identify peculiarities in relation with the various exposure typologies, including industrial, urban, and rural. Beyond, an extensive statistical work based on PCA was carried out to identify component factors in relation with known emission sources and further to estimate their relative contributions.

Materials and methods

Study area

The study area is located around Fos-sur-Mer, 50 km west from Marseille (France). It covers about 30 × 30 km and is populated by approximately 180,000 inhabitants. It is characterized by a very contrasted environment, including numerous major atmospheric emission sources, as it hosts the main maritime industrial zone in France, including several heavy industry activities (oil refining, petrochemistry, chemistry, coke production and steel industry, cement plant, household and industrial waste incineration units) and world-leading maritime terminals (containers, ore, oil, gas, cereal). Furthermore, agricultural activities in the northern part of the area may be locally significant where large vineyards and olive fields predominate (by sites *u5*, *u6*, and *u7* as well as *r2*, *r3*; Fig. 1). Elsewhere, hay is the main culture among Mediterranean fruits. It remains obvious that road traffic emissions should be considered in urbanized areas and next to major highways. On the other hand, this territory is flanked by wide natural areas, the Plain of Crau and Alpilles mountains (300 to 500 m a.s.l.) to the north, and the Camargue nature reserve to the west, as well as marine territories to the east (Berre Lagoon) and south (Mediterranean Sea), the shipping channels and anchorages being mainly located within the Gulf of Fos. It is very flat with only a few gentle hills (< 200 m a.s.l.) between sites *u1* and *u2*, and *u3* and *u4* (Fig. 1).

The Fos-sur-Mer area receives Mediterranean climatic conditions, where the mean temperatures range from 2.8–11.2 °C in January to 18.9–30.2 °C in July (average low–high temperatures). Rainfall usually concentrates in autumn and spring, often heavily, cumulating annually 554.3 mm in the 1981–2010 period distributed into an average of 53.5 rainy days (calculated over the 1981–2010 reference period from the Météo-France data of the Istres station, noted “A” in Fig. 1).

Sampling and preparation

The present sampling campaign represents the fourth consecutive yearly campaign of a long-term program (Dron et al. 2016) and lasted for 1 week overall in January 2017. Assuming an integration by lichens of contaminants over at least several weeks or months (Nimis et al. 2002; Augusto

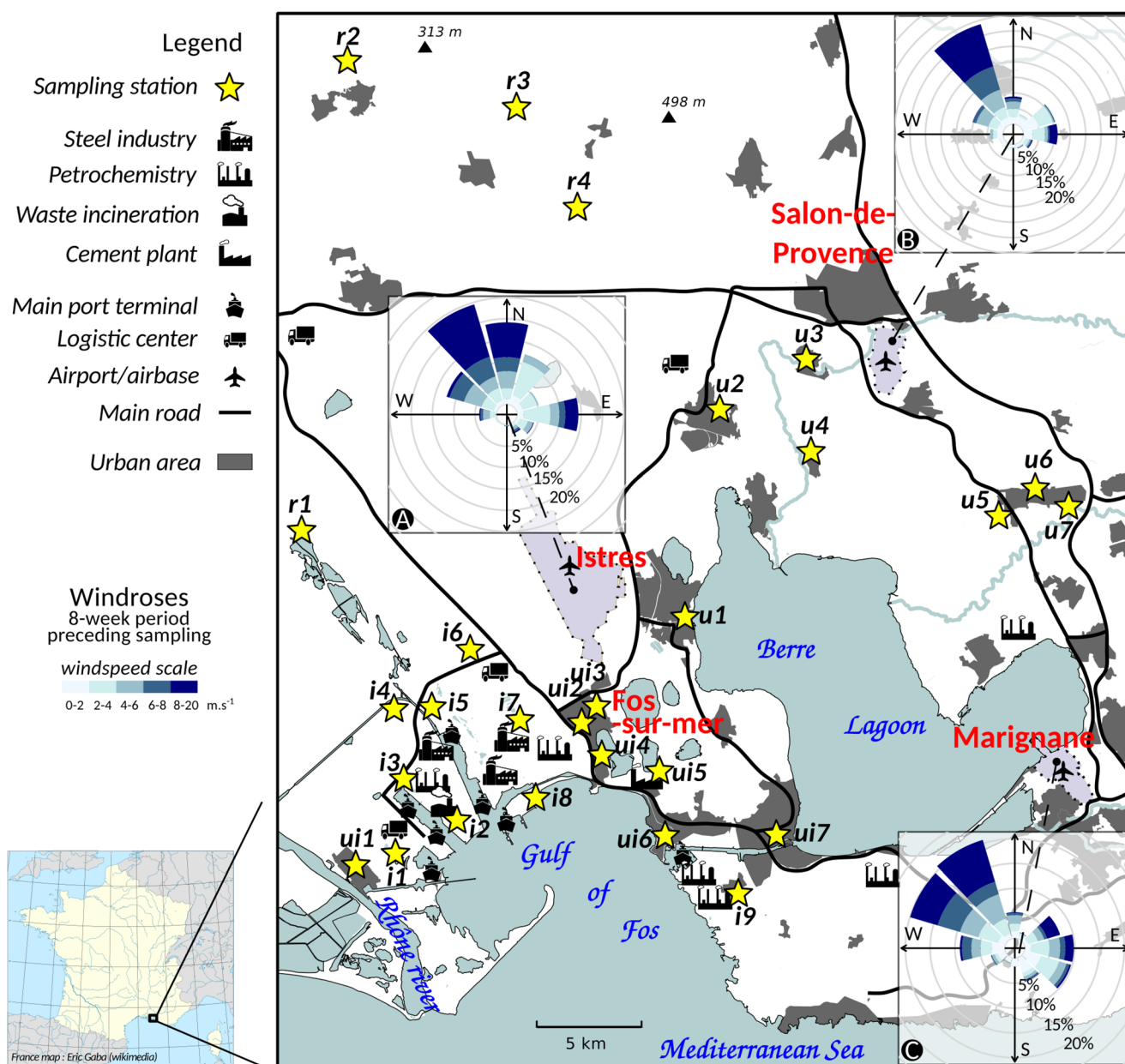


Fig. 1 Detailed map of the study area with the 27 sampling sites and wind conditions (hourly data from Météo-France)

et al. 2009), it could be considered that all the area was submitted to comparable climatic conditions. During the 8 weeks preceding sampling, mean temperatures and relative humidity were 9.3–10.2 °C and 73–76%, respectively, and total precipitations ranged from 84 to 131 mm in the three major meteorological stations located in the area. The period was also dominated by similar NW and E winds throughout the area, as shown in Fig. 1 (all meteorological averages are based on hourly data from Météo-France).

The 27 sampling sites have been positioned away from main road sides and culture fields to avoid direct contamination. They were chosen to form a representative panel of the various exposures offered in the study area, in order

to explore the specificities of their potential signatures, and classified into four categories according to their environment and distance to the closest major industrial installation:

- *Industrial*: By heavy industries (0.5 to 5 km) but away from urban centers (numbered from *i*1 to *i*9)
- *Urban-industrial*: Urban environments near (< 5 km) industrial installations (numbered from *ui*1 to *ui*7)
- *Urban*: Within cities more than 5 km away from major industries (numbered from *u*1 to *u*7)
- *Rural*: Rural areas away from any urban center, major road, or industry (numbered from *r*1 to *r*4)

The quality of the results in lichen biomonitoring is dependent on the sampling strategy and local significant variations. In particular, the sampling variability can be related to the dimensions of the sampling sites, reaching up to 40–60% for example in a 100-km² mesh, but kept under 35% when narrower (Adams and Gottardo 2012). In the present study, the site parcels covered approximately 200 m² areas and should thus limit local variations considering the whole study area of almost 1000 km². The sampled lichens were collected from all sides of five to ten tree trunks (mainly poplar, tamarix, ash, oak ...) and at least 1 m above the ground to avoid the potential influence from soil particles. It should be noted that the tree species supporting the collected lichens (phorophytes) may have an influence on the contaminant bioaccumulation. However, this is generally limited, in particular when the sampling sites are not totally opposing in terms of phorophyte species like it was the case here or in other studies (Bajpai et al. 2009; Daimari et al. 2013).

Whole *X. parietina* thalli were collected using ceramic knives to separate the lichen from their phorophytes (Fig. S1) until the sample reached at least 10–15 g wet weight. The sampled thalli were placed in Nalgene® flasks brought to the laboratory in less than 3 h. They were then stored away from light at 4 °C for a maximum of 48 h and sorted with non-metallic material (ceramic and PS) to remove remaining dust, barks from their phorophytes, and unwanted species. They were then stored at –30 °C for at least 24 h, freeze-dried for 72 h (–55 °C/0.035 mbar, Christ-Alpha 1-4LD) and finally ground in a ball mill (1.5 min, 25 Hz, Retsch MM 400 equipped with ZrO₂ beads and capsules), leading to homogenized fine-powder composite samples.

Chemical analyses

For each chemical analysis procedure, the full chemical references and the complete results of quality controls are provided in Supplementary Information S1, Table S1 (metals), Table S2 (PAHs), and Table S3 (PCBs).

Metals and metalloids

About 300 mg of the homogenized samples were dissolved in a mixture of nitric acid (7.5 mL, 65% v/v) and hydrochloric acid (2.5 mL, 37% v/v) for the determination of 18 metals and metalloids (Ag, Al, As, Cd, Co, Cr, Cu, Fe, Hg, Mn, Mo, Ni, Pb, Sb, Sn, Tl, V, Zn). Mineralization was carried out using a microwave system (Ethos advanced μ -wave LabStation) at 180 °C for 20 min. The sample was then diluted in ultrapure water to 50 mL and analyzed by ICP-MS (ICAP Q, ThermoElectron).

Mercury (Hg) was prepared apart, by dissolving 300 mg in nitric acid (5 mL, 65% v/v) and adding a solution of gold (100 μ L at 10 μ g L⁻¹) to form a Hg–Au complex and avoid

the volatilization of Hg. This solution was allowed to stand for 72 h at room temperature before analysis using ICP-MS. Duplicates were prepared and analyzed for all samples, from the homogenized powder. Briefly, the quality control was based on the determination of concentrations in lichen and ray grass-certified materials, which were all within the recommended values. Detection limits range from 0.05 to 0.1 mg kg⁻¹ and standard deviations from 5% to 10%. Further details regarding metal elements analysis are provided in the Supplementary Information S1 and Table S1.

PAHs

The analysis of polycyclic aromatic hydrocarbons (PAHs) focused on the 16 compounds from the US Environmental Protection Agency (USEPA) priority list, naphthalene (Nap), acenaphthylene (Acy), acenaphthene (Ace), fluorene (Flu), phenanthrene (Phe), anthracene (Ant), fluoranthene (FlA), pyrene (Pyr), benzo(a)anthracene (BaA), chrysene (Chr), benzo(b)fluoranthene (BbF), benzo(k)fluoranthene (BkF), benzo(a)pyrene (BaP), benzo(ghi)perylene (BPe), dibenzo(ah)anthracene (DBA), and indeno(1,2,3-cd)pyrene (IPy), and was adapted from Sarrazin et al. (2006). Freeze-dried ground samples (~0.5 g) were extracted with 20 mL acetone in an ultrasonic bath (2 × 15 min at 40 Khz and 200 W, JP Selecta). It was left for 12 h at room temperature, and a 10 mL aliquot of the supernatant was filtered through a 9-cm glass microfiber filter (pore size 2.7 μ m, Grade GF/D, Whatman). Then, 15 mL of ultrapure water was added, and the solution was passed through a 1-g C-18 cartridge (6 mL volume, Bond Elut, Agilent) previously wetted with 5 mL acetone and further conditioned with 5 mL of acetone/water 40:60 (v:v). The column was air dried for 20 min, and the PAH was eluted with 3 × 1 mL acetone followed by 2 × 1 mL methanol. They were finally analyzed by HPLC (Waters 2695 Alliance) equipped with UV and fluorescence detectors (Waters 2487 and 2475) and a C-18 column (Waters 5 μ m HAP 4.6 × 250 mm). Two to three replicates from the pooled powder samples were prepared and analyzed. In the absence of lichen-certified material, the analytical reliability was determined as the individual congeners recoveries which were calculated from a spiked test sample collected by station *i6* and ranged from 73% to 100%. The detection limits were 1 μ g kg⁻¹, and the mean deviations based on the replicate analyses of the field samples ($N=27$) ranged from 3% to 16%. More details on the analytical method and quality tests are given in the Supplementary Information S1 and Table S2.

PCDD/Fs

The determination of PCDD/F concentrations concerned the 17 congeners from the WHO list (Van den Berg et al. 2006) in

all samples except sites *u5*, *u6*, and *u7*, and was performed by La Drôme Laboratoire (Valence, France).

The ASE extraction (ASE300, Dionex) was carried out with dichloromethane/acetone (50/50, v/v) and by running 3 cycles of 5 min at 120 bar and 100 °C. The samples were concentrated to 10 mL and treated with copper (12-h stirring). The extracts were spiked with corresponding ¹³C-labeled compounds and acidified with 2 mL of concentrated sulfuric acid (98%). Then, the solution was purified using Florisil 3%, and the PCDD/Fs were eluted using toluene. A second purification was performed using carbon-celite 18%. PCDD/Fs were separated by GC (Agilent 7890A) equipped with an apolar column (RTXPCB 40 m × 0.18 mm × 0.18 μm). The temperature program was as follows, 140 °C (hold for 0.6 min) increased to 210 °C at a rate of 35 °C min⁻¹; to 250 °C at 1.6 °C min⁻¹; and finally to 310 °C at 3.5 °C min⁻¹. The samples were detected by HRMS after electronic impact ionization (Jeol 800D). Details concerning the analytical quality control for the determination of PCDD/F can be found in the Supplementary Information S1.

PCBs

PCBs were determined for the six indicators (PCBi 28, 52, 101, 138, 153, and 180) and 12 dioxin-like congeners (PCB-DL 77, 81, 105, 114, 118, 123, 126, 156, 157, 167, 169, and 189) defined in the European regulations (European Commission 2011).

Quantitative analyses of PCBs were performed following previously described procedures (Wafo et al. 2006). Briefly, the samples (0.5 g) were Soxhlet extracted with hexane (16 h at 45 °C) and purified with concentrated sulfuric acid. The extracts were then submitted to an activated alumina solid phase extraction and eluted with hexane (fraction A). An additional extraction using activated silica and hexane elution (fraction B) was achieved to recover residuals of eight PCB-DLs (77, 81, 114, 126, 156, 157, 169, 189). Fraction A was determined by GC/ECD equipped with a ⁶³Ni detector (HP 6890), and fraction B by GC/MS (Agilent 6890 N). Two to three replicates of the homogenized powder were prepared and analyzed. Shortly, the individual congener recoveries were calculated from a spiked test sample collected by station *i6* and ranged from 70 to 124%. The detection limits were 0.01 μg kg⁻¹, and the mean deviations based on the replicate analyses of the field samples (*N* = 13) ranged from 12 to 29%, except PCB105 (66.9% in average) due to levels that were all near its detection limit in the samples. More details on the analytical method and quality tests are given in the Supplementary Information S1 and Table S3.

Data analysis

The water content was determined by deducting the sample weight before and after they were freeze-dried, and the contaminant concentrations in *X. parietina* strictly refer to their dry weight in order to avoid any influence due to water content variability (8% to 30% depending on sampling conditions). The undetected metallic elements Hg and Ag as well as Tl (detected in two sites only) were not included in the data analyses.

Statistical analyses and graphical representations were performed with the statistical software R version 3.2 (R Core Team 2016) and the vector graphics editor Inkscape. Compounds which were not detected (nd) or below the limit of quantification (< lq) were considered as the limits of detection (ld).

Principal component analyses (PCA) were carried out assuming missing values as the mean of all other values for the factor (applies to 14 PCBs and 3 PCDD/F samples not measured) and considering standardized data (z-scores). It was preferred here to the more constrained analyses, such as positive matrix factorization (PMF) or non-negative matrix factorization, in order to identify in the first place the contaminant signatures that could be drawn in relation with the main atmospheric emissions that are consistent in the study area.

The hierarchical cluster analysis of metallic elements was realized using standardized data also, employing Euclidean distances and the ward.d2 criterion (Murtagh and Legendre 2014; R Core Team 2016).

Significant differences were considered according to the one-way ANOVA results and post hoc Tukey's tests (confidence level = 0.95). The latter was realized using the "HSD.test" function from the "agricolae" package (de Mendiburu 2017).

Results and discussion

Metals and metalloids

Many metals and metalloids have their concentrations above the recently calculated French background levels reported by Agnan et al. (2015) and Occelli et al. (2016), even in the least exposed locations (Table 1). In particular, they both indicate lower backgrounds than the present rural concentrations for As (under 0.85 mg kg⁻¹), Cr (under 4.23 mg kg⁻¹), and Sb (under 0.30 mg kg⁻¹). The element Fe background, only reported by Agnan et al. (2015), is also much lower (1330 mg kg⁻¹) than what was measured here in rural samples, representing here the lowest Fe levels. Globally, the concentrations are in the range of what observed in the previous years (Dron et al. 2016), and of other industrial environments, where the literature generally reports the highest

Table 1 Mean concentrations and standard deviations for metals and metalloids (mg kg⁻¹), PAHs and PCBs (μg kg⁻¹), and PCDD/Fs (ng kg⁻¹) measured in *X. parietina* samples according to site categories (N = 9; N = 7; N = 7; N = 4 in industrial, urban-industrial, urban, and rural categories, respectively). Different letters between brackets indicate significant differences between categories, as a result of ANOVA and post hoc Tukey's test ("a" or "b"; both letters "ab" specifies that the value is not significantly different than "a" and "b")

	Industrial	Urban-ind.	Urban	Rural
Al	3661 ± 1554 (a)	3488 ± 1082 (a)	2953 ± 969 (a)	2198 ± 829 (a)
V	11.7 ± 4.4 (a)	7.16 ± 1.88 (b)	4.71 ± 1.24 (b)	3.50 ± 0.64 (b)
Cr	30.0 ± 16.6 (a)	14.9 ± 6.3 (b)	7.40 ± 1.30 (b)	6.33 ± 1.19 (b)
Mn	194 ± 116.7 (a)	93.0 ± 13.5 (b)	62.4 ± 16.7 (b)	54.2 ± 12.4 (b)
Fe	14,114 ± 11,786 (a)	5508 ± 1007 (ab)	3632 ± 1050 (b)	3521 ± 528 (b)
Co	1.24 ± 0.42 (a)	1.13 ± 0.17 (a)	0.87 ± 0.21 (a)	0.78 ± 0.19 (a)
Ni	14.0 ± 11.1 (a)	13.6 ± 7.1 (a)	9.79 ± 4.9 (a)	7.00 ± 2.7 (a)
Cu	17.9 ± 11.1 (a)	13.0 ± 5.6 (a)	25.5 ± 27.5 (a)	10.3 ± 1.9 (a)
Zn	70.9 ± 49.6 (a)	46.4 ± 11.0 (a)	32.3 ± 7.8 (a)	28.6 ± 10.3 (a)
As	2.39 ± 1.12 (a)	1.61 ± 0.72 (a)	1.17 ± 0.80 (a)	1.10 ± 1.01 (a)
Mo	13.9 ± 28.5 (a)	1.44 ± 0.48 (a)	1.37 ± 0.66 (a)	1.20 ± 0.18 (a)
Cd	0.48 ± 0.24 (a)	0.39 ± 0.16 (ab)	0.21 ± 0.04 (ab)	0.23 ± 0.05 (b)
Sn	4.40 ± 2.37 (a)	3.93 ± 1.32 (a)	4.33 ± 2.60 (a)	4.15 ± 1.01 (a)
Sb	1.71 ± 0.61 (a)	2.01 ± 1.97 (a)	1.20 ± 0.22 (a)	0.78 ± 0.21 (a)
Pb	21.4 ± 9.4 (a)	14.4 ± 4.6 (ab)	9.26 ± 3.09 (b)	7.50 ± 2.09 (b)
ΣPAH	904 ± 263 (a)	784 ± 92 (ab)	675 ± 40 (b)	570 ± 14 (b)
ΣPCDD ¹	51.3 ± 42.4 (a)	46.9 ± 23.6 (a)	58.5 ± 41.8 (a)	22.5 ± 5.3 (a)
ΣPCDF ¹	64.4 ± 99.0 (a)	17.1 ± 7.8 (a)	17.3 ± 10.7 (a)	11.5 ± 2.6 (a)
PCDD/F _{ITTEQ} ¹	3.83 ± 2.70 (a)	1.77 ± 0.38 (a)	2.28 ± 0.71 (a)	1.90 ± 0.69 (a)
PCB _S ²	8.23 ± 2.47 (a)	6.96 ± 0.58 (a)	9.51 ± 2.09 (a)	6.53 ± 1.34 (a)
PCB-DL _S ²	1.87 ± 0.28 (ab)	1.34 ± 0.27 (b)	2.85 ± 0.70 (a)	1.92 ± 0.14 (ab)

¹ N = 4 in the urban category

² N = 3; N = 2; N = 6; N = 2 in industrial, urban-industrial, urban, and rural categories, respectively

concentrations as for examples Al (350–6700 μg kg⁻¹), V (2–100 μg kg⁻¹), Fe (1200–28,000 μg kg⁻¹), or As (0.4–9 μg kg⁻¹) (Hissler et al. 2008; Demiray et al. 2012; Occelli et al. 2013). Because Hg and Ag were never detected, and Tl only in two industrial sites (0.10–0.11 mg kg⁻¹), they were not reported in Table 1.

The highest concentrations of all elements are found in industrial areas, except Cu and Sb (Fig. S2). In more detail, the industrial category presents significantly higher concentrations for V, Cr, Mn, Fe, Cd, and Pb compared to urban and rural environments (Table 1, Fig. S3). For these elements, but also Al, Co, Ni, Zn, As, and Mo, the industrial samples reveal much greater disparities compared to urban or rural sites, showing the complexity and the diversity of industrial exposures at the local scale.

Even though the prominence of Fe, Al, and Mn (Table 1) in the lichen samples is often attributed to crustal dust inputs or road traffic (Agnan et al. 2015; Liu et al. 2016), the extreme levels and the strong discrepancies observed here clearly point out steel activities and possibly ore terminals as predominant contributors. The strong bioaccumulation of metallic elements in lichens reflects here the major impact of the steel industry emissions which are characterized by high Fe and Mn inputs as recently shown in the same area (Sylvestre et al. 2017). Hierarchical clustering was applied to metallic elements

(standardized data), aiming to split these variables into groups with similar behavior among the area under study (Reimann et al. 2008). The resulting dendrogram illustrates how the variabilities of Mn and Fe are associated, along with Cd and in a lesser extent As which may also be related to steel industry (Fig. 2). On the other hand, Al seems more specific to ore terminal activities, as recently documented locally in PM2.5 (Sylvestre et al. 2017). In contrast with Fe, Al is more concentrated in sites *i2* and *i3* by the main ore terminals, rather than sites *i5* to *i8* surrounding the steel industrial complex (Fig. S2), supporting this assumption. In addition, other substantial sources, such as the aluminate cement plant by site *ui5* (Fig. 1) may contribute to the bioaccumulation of Al (high levels in sites *ui5* and *ui6*).

The elements V, Zn, and Pb are also well-clustered together (Fig. 2). According to recent works, these are more representative of chemical, petrochemical, and oil refinery emissions (Sylvestre 2016). Molybdenum (Mo) stands out as it is used in only one chemical plant in the Fos-sur-Mer area (Dron and Chamaret 2015), located between sites *i2* and *i3* which are the two Mo outliers (Figs. S2 and S3).

On the contrary, the elements Cu, Sn, and Sb are of comparable levels in lichens from all environments. The similar behavior obtained for these elements was already observed in literature (Veschambre et al. 2008; Agnan et al. 2015;

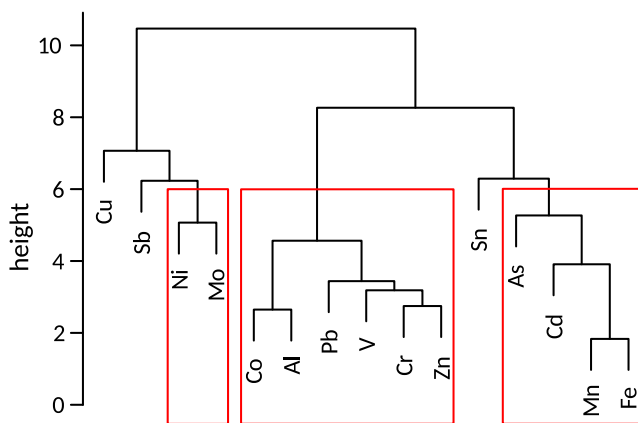


Fig. 2 Hierarchical clustering of the metal and metalloid standardized levels (z-scores, $N=27$)

Boonpeng et al. 2017), and the present results show a significant correlation between Cu and Sb, $R=0.62$; $p=0.001$ (Pearson excluding outliers). Cu and Sb are known to be characteristic of road traffic emissions from brake wear (Sternbeck et al. 2002; Lough et al. 2005). Also, they precisely present here their highest concentrations in the most busy city centers (sites *ui6* and *ui7*, Fig. S2). Other elevated levels of Sb occur in sites *i2*, *i3*, and *i4* also suggesting a significant contribution from industrial activities, while Cu is particularly high in sites *u5*, *u6*, and *u7* where the use of Cu-based fungicides can be significant (extensive vineyards and olive tree fields).

Polycyclic aromatic hydrocarbons (PAHs)

All of the 16 PAHs from the USEPA priority list were detected in all samples. The samples collected in the industrial and industrial-urban areas are the most concentrated (ΣPAH ranging from 569 to 1417 $\mu\text{g kg}^{-1}$ and from 683 to 949 $\mu\text{g kg}^{-1}$, respectively), significantly above the urban and rural categories (ΣPAH ranging from 624 to 728 $\mu\text{g kg}^{-1}$ and from 549 to 582 $\mu\text{g kg}^{-1}$, respectively), highlighting the great influence of the industrial activities on the local PAH atmospheric concentrations (Table 1). Similarly, the disparities observed for ΣPAH increase strongly from rural and urban locations (RSD = 2.5% and 5.9%, $N=4$ and 7, respectively) to industrial (29.1%, $N=9$).

In comparison, the mean values measured in *X. parietina* thalli collected during the 2011–2013 period in the same sites (Dron et al. 2016) were in the same range for the industrial sites ($\Sigma\text{PAH}=1199\pm 307 \mu\text{g kg}^{-1}$) and the industrial-urban samples ($\Sigma\text{PAH}=650\pm 38 \mu\text{g kg}^{-1}$), but two to three times lower in urban and rural areas ($\Sigma\text{PAH}=265\pm 42 \mu\text{g kg}^{-1}$ and $\Sigma\text{PAH}=200\pm 62 \mu\text{g kg}^{-1}$, respectively). The difference observed with the 2011–2013 period is particularly meaningful in urban and rural environments. This could reflect a significant impact of biomass burning and residential heating emissions and will proportionally affect more the urban and rural

categories than the industrial ones which present comparatively higher ΣPAH levels induced by industrial emissions. The present sampling was held later in January, compared to the previous years carried out in Nov–Dec with warmer late autumn conditions (mean temperatures 2 months before sampling were 2 to 7 °C below the previous year campaigns). Accordingly, the local seasonality of the biomass burning contribution in PM_{2.5} does not increase consistently before the end of November in the Fos-sur-Mer region (Sylvestre 2016). Kodnik et al. (2015) measured higher ΣPAH levels in urban sites in winter as well and noted that, on the contrary, the influence of small industrial units could be enhanced in summer compared to urban and rural environments. However, the upper-end concentrations observed here are much higher than what reported in other foliose lichens from urban environments, still supporting the hypothesis of a strong industrial impact on ΣPAH concentrations in lichens (Domeño et al. 2006; Augusto et al. 2009; Van der Wat and Forbes 2015).

The distribution of the PAH congeners is quite homogeneous throughout the study area. Some compounds still show noticeable variations among their exposure, as Nap and Ipy which relative contributions to ΣHAP are higher in industrial samples, or on the contrary Ant, BaA, and Chr which relative contributions to ΣHAP are higher in rural samples (Table S4). As shown in Fig. 3, the profiles are dominated by the 3-rings PAHs (Phe, Acy, and Ace; $31\pm 11\%$, $20\pm 9\%$, and $14\pm 10\%$, respectively), as observed in most lichen samples worldwide (Van der Wat and Forbes 2015; Dominguez-Morueco et al. 2017). The three-ring congeners Ace and Acy are the most reactive PAHs, explaining their higher contributions under cold winter conditions (Atkinson and Arey 1994; Dimashki et al. 2001). However, such relations with atmospheric reactivity still require complementary works to elucidate.

Dioxins and furans

As for PAHs, all the PCDD/F congeners were detected in all samples. The great disparity in contaminant concentrations within the industrial category is here again illustrated, gathering the lowest as well as the highest levels in the studied sites

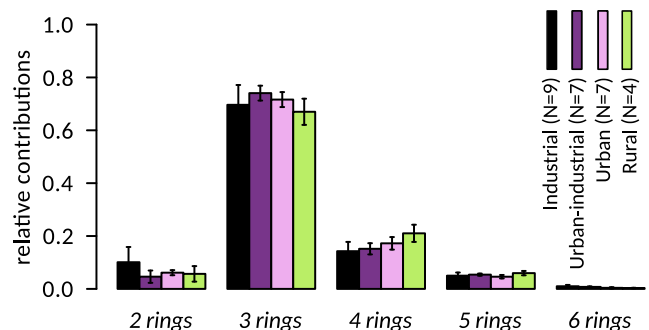


Fig. 3 Distribution of PAH according to their number of aromatic rings and the site typology

(Table 1, Fig. 4a). The industrial concentrations range from 26.2 to 472 ng kg⁻¹ while urban and urban-industrial samples have narrower ranges, ΣPCDD/F from 43.0 to 154 ng kg⁻¹ and from 34.5 to 107 ng kg⁻¹, respectively. Rural samples are very homogeneous and below all other categories, ΣPCDD/F ranging from 27.3 to 42.2 ng kg⁻¹. Globally, the concentration levels are comparable to previous years' mean values throughout the area, which were ranging from 108 ± 88 ng kg⁻¹ to 156 ± 156 ng kg⁻¹ (Dron et al. 2016). On the other hand, they are quite higher than what were obtained by Augusto et al. (2015) in *X. parietina* since 2009 in a lower-scale industrial zone (Setubal, Portugal). However, the evolution of the ΣPCDD/F concentrations during the 2011–2014 time span does not show any clear trends in the Fos-sur-Mer region and suggests constant atmospheric levels at this scale.

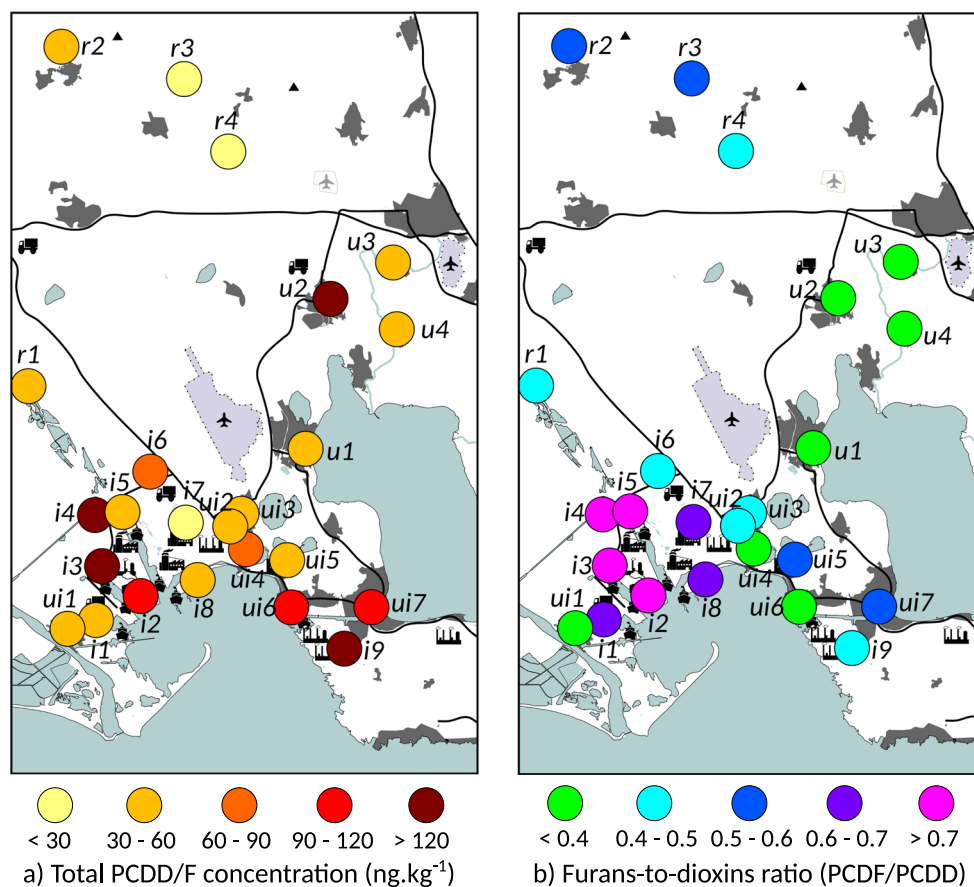
In all the investigated sites, octa- and heptachlorinated dioxin and furan congeners were largely prevailing, accounting for 60 ± 11% and 20 ± 5%, respectively (Table S5), similarly to the last observations in *X. parietina* reported by Augusto et al. (2015). The PCDD/F atmospheric concentrations depend on primary emission levels, atmospheric reactivity, and gas/particle partitioning. Also, the atmospheric reactivity of PCDD/Fs decreases when the number of chlorine atoms becomes higher, and at equal chlorination degrees, PCDFs have longer atmospheric lifetimes than PCDDs (Atkinson 1996).

However, the spatial distribution of PCDD/Fs according to their chlorine content did not differ significantly, contrarily to the furan-to-dioxin ratios (PCDF/PCDD) indicating that the differences observed in the PCDD/F profiles are not due to atmospheric reactivity. The PCDF/PCDD ratios range from 0.25 to 2.15, with particularly elevated values in the industrial sites *i2* to *i5*, which are surrounded by incineration facilities and other industries (Fig. 4b). On the contrary, PCDFs are notably low in all the urban sites, where PCDF/PCDD ratios range from 0.28 to 0.37, suggesting that the main PCDD/F local sources (presumably industrial and urban) lead to different patterns in lichen, either PCDF or PCDD predominance, respectively. Interestingly, rural sites show intermediate and homogeneous PCDF/PCDD values (0.48 to 0.57), which could reflect a substantial industrial contribution despite low PCDD/F concentrations (Fig. 4), as these sites are not exposed to any other source of PCDD/Fs in their vicinity. Similarly, PCDD/F industrial patterns were also recently observed in lichen samples having low concentrations, collected nearby a cement plant in Portugal (Augusto et al. 2016).

Polychlorinated biphenyls

Among the 18 PCBs measured in 13 of the 27 investigated sites, the 6 indicators (PCB_s) and 3 of the 12 PCB-DL were

Fig. 4 Comparative spatial distributions of (a) PCDD/F total concentrations (ng kg⁻¹) and (b) furans-to-dioxins ratios (N = 24)



found in all sites while the other 9 PCB-DLs were never detected. The sum of the concentrations for these 18 PCBs ranges from $7.1 \mu\text{g kg}^{-1}$ (industrial site *i3*) to $16.4 \mu\text{g kg}^{-1}$ (urban site *u5*), with PCBs accounting for 72 to 87% (Table 1).

The samples collected in urban locations have the highest ΣPCB levels (ranging from 10.1 to $16.4 \mu\text{g kg}^{-1}$), followed by those from industrial sites (7.1 to $12.4 \mu\text{g kg}^{-1}$). The spatial distribution of PCB concentrations in lichen suggests a larger implication of urban sources (residential heating, road traffic), contrasting with the industrial predominance observed for the other contaminant categories. However, literature concerning the accumulation of PCBs in lichen is particularly scarce and is limited to fruticose species, causing a lack of reference points. The results observed here are 1 to 3 orders of magnitude higher than in remote areas such as the Tibetan plateau or Antarctica, respectively (Park et al. 2010; Zhu et al. 2015), and about 5 to 10 times higher than the levels reported by Protano et al. (2015) around a solid waste incinerator in Italy.

The pentachlorinated PCBs are the most abundant congeners, representing $40.3 \pm 7.7\%$ on average of the ΣPCB . Among them, the PCB 101, PCB 105, and PCB 118 have higher contributions in urban and rural samples, while the PCB 180 reveals a stronger industrial influence. The other compounds were relatively homogeneously distributed, regardless of the exposure typologies (Fig. 5, Table S6). The reactivity of PCBs in the atmosphere essentially involves OH radical addition which kinetics is faster for the lower degrees of chlorination, leading to a longer lifetime of highly chlorinated congeners, lasting from several days to months, respectively (Atkinson 1996; Anderson and Hites 1996). The preeminence of PCBs having an intermediate degree of chlorination, and more importantly the homogeneous concentrations and profiles throughout the study area indicate that all the samples were roughly exposed to the same sources of PCBs. Considering the nature of the investigated locations, spread out over very different typologies, a regional-scale contribution is thus probably substantial.

Characterization of exposure typologies from contaminant profiles

The industrial proximity induces strong contrasts compared to the more urban and rural environments, either in terms of total contaminant class concentrations (metals, PAHs, PCDD/Fs) or congener and element signatures (metals, PCDD/Fs). The sampling of all sites lasted for only 1 week, and the atmospheric reactivity conditions were comparable among the whole study area and along the sampling period at the time scale of lichen bioaccumulation. During the sampling week, hydroclimatic conditions were indeed homogeneous, with mean temperatures ranging from 7.2 to $8.2 \text{ }^\circ\text{C}$ and humidity from 70% to 79%, and total precipitations from 0 to 0.4 mm (Meteo-France data from weather stations A, B, and C, Fig. 1). Moreover, the climatic conditions were quite homogeneous in the three weather stations at least during the approximative accumulation time of lichens (8 weeks), as indicated in the “Sampling and preparation” section. Thus, even though local climatic phenomena may still have some incidence, the bioaccumulation of contaminants in the sampled lichens should principally depend on their different exposure to emission sources. Also, particular emission sources may generate specific contaminant profiles, which could be retrieved in lichen samples. Multivariate analyses, and more particularly principal component analyses (PCA), are well suited to characterize potential relationships between a wide set of variables and observations together and are commonly used in atmospheric source apportionment studies applied to volatile organic compounds or particulate matter composition (Viana et al. 2008; Reimann et al. 2008). They also offer various valuable graphical opportunities to describe the results as for example geographical mapping of the identified groups (principal components). It was also preferred to the common PMF analysis, as a first step in order to identify signatures and patterns potentially implying numerous factors (Christensen et al. 2018). Also, specific contaminant patterns could have been sorted from the PCA applied to all 27 samples, the 15 ubiquitous metals,

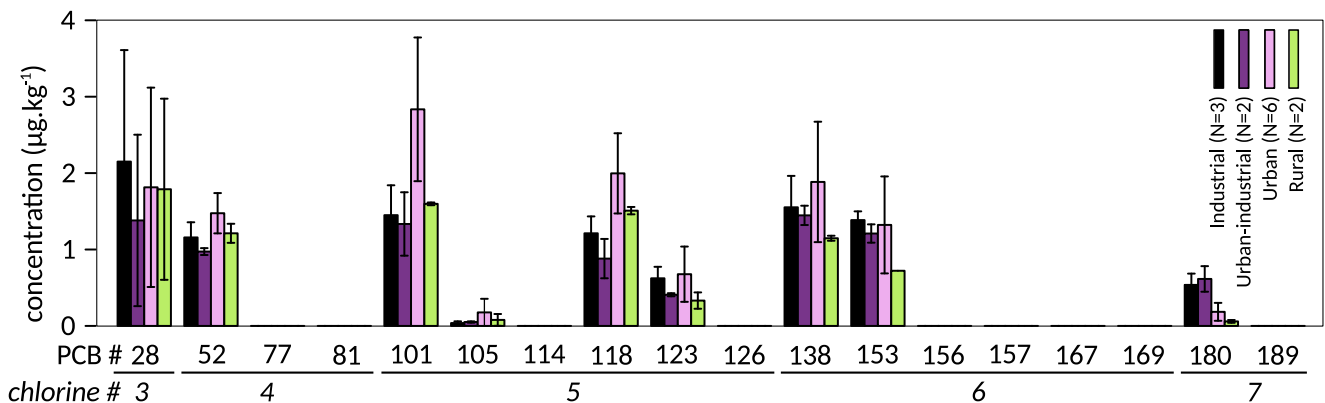


Fig. 5 PCB congener mean concentrations according to the site typology. Error bars correspond to min/max when $N=2$ and standard deviations when $N>2$

and 12 organic classes (5 PAH classes according to their number of rings, PCDD, and PCDF, 5 PCB classes according to their number of chlorine atoms). In particular, the profiles of the sorted factors (i.e., contaminants) show peculiarities in several components which are very relevant considering what expected from local emission sources (Fig. 6a).

The main component (explaining 34.1% variability) includes all metals, PAHs, and PCDD/Fs. Regarding the mapping of the observed coordinates of this first component (Fig. 6b), it suggests a global industrial contribution which is particularly high in all industrial sites (except site *i1*) and shows also strong inputs in the neighboring cities (sites *ui1*, *ui2*, *ui6*, and *ui7*).

The second component is more specific and explains 13.5% of the variability. It is exempt of organics and is driven by the metallic elements Sn, Fe, Mn, Cd, and As. Among what has been determined here in the “Metals and metalloids” section, these elements were recently identified locally as atmospheric markers of the steel industry

emissions (Sylvestre et al. 2017). More generally, numerous metals and particularly Fe and Mn are usually associated to steel industry (Pernigotti et al. 2016); nevertheless, Mn can also result from vehicular traffic emissions. However, the hypothesis of a prominent industrial origin is still supported by the geographical distribution of this component around the steel industry installations (sites *i5* and *i8*), which also impacts the nearby cities (sites *ui1*, *ui2*, *ui4*). Its high level in more rural locations illustrates the potentially elevated relative contributions in less contaminated samples (Fig. 6), as observed for the PCDF/PCDD ratios (Fig. 4).

The high specificity of molybdenum (Mo) emissions, identified as a specific marker of a single chemical industry installation (Dron and Chamaret 2015), generates a distinct component (12.6% of the variability) which also includes PCDD/Fs, but no other contaminants. This component appears spatially associated to this industrial activity along with the other co-located industries, including two waste incinerators that can

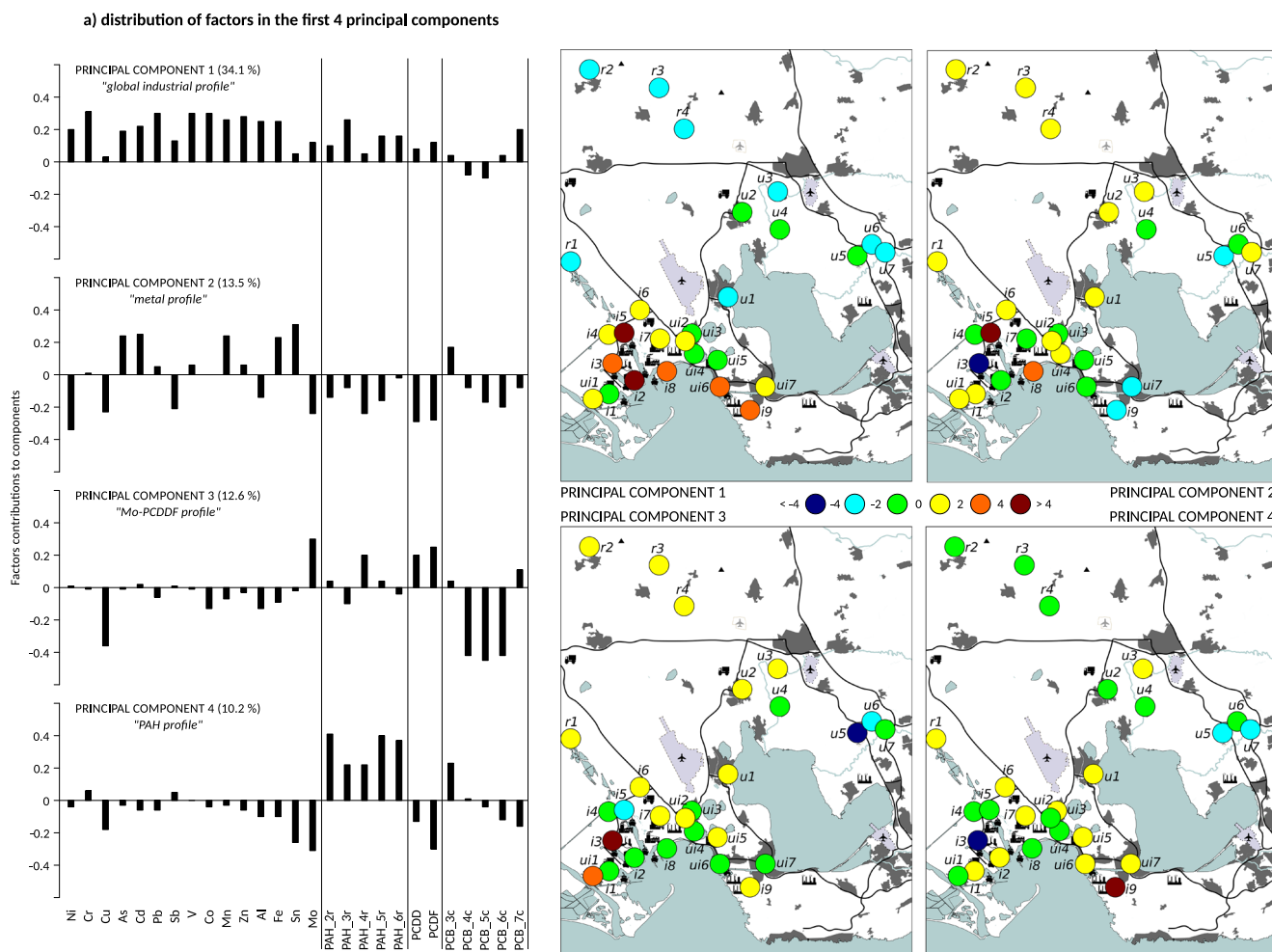


Fig. 6 Principal component analysis of the contaminant levels through the study area (standardized data, $N = 27$). (a) Detailed distributions of factors (i.e., contaminants) in the first four principal components and (b)

mapping the coordinates of the individuals (i.e., sampling sites) in the factorial planes of the same four components

produce substantial PCDD/F emissions (Fig. 6). Among its great incidence on site *i3* nearby, the influence of this component spreads out to the rural areas, similarly to the steel industry component and the geographical distribution of the PCDF/PCDD ratios (Fig. 4). Again, this suggests a significant relative input in these more distant sites which are not directly exposed to other particular sources.

A PAH exclusive component contributes to 10.2% of the variability and is exempt of any metallic element and PCDD/F. Such profiles are generally attributed to biomass burning in atmospheric source apportionment studies (Viana et al. 2008; Pernigotti et al. 2016). Here, the lichen PAH component appears to be homogeneous across the study area, which is consistent with a regional impact of biomass burning sources distributed in urban (heating purposes) and rural environments (heating, stubble-burning). Logically, this component is also influenced by the main petrochemical complex in the study area, regarding its specifically high level in site *i9*, possibly evidencing some mixture of biomass burning and petrochemistry factors here.

The Sb and PCDD contaminants contribute intensively in the seventh component, which explains 3.8% of the overall variability. These compounds (see the “Metals and metalloids” and “Dioxins and furans” sections) suggest an urban and road traffic-related profile, in accordance with the fact that the highest positive coordinates are obtained for six urban sites (*ui6*, *ui7*, *u1*, *u2*, *u3*, and *u7*) along with sites *i4*, *i5*, and *r1*.

Even though a potentially high degree of mixing of sources remains in the components, the sum of those which were mainly associated to industrial emissions exceeds 60%, corroborating the strong influence of industrial emissions among the bioaccumulation of atmospheric contaminants in lichens, even when located 20–30 km away from these sources where total concentrations are more limited.

Conclusions

The analysis of metals, PAHs, PCDD/Fs, and PCBs in 27 lichen samples from contrasted environments (industrial, urban, rural) located around a major industrial and portuary zone from South of France revealed specificities related to the sampling site typology. Approaching industrial installations generally lead to much higher concentrations, but also to increasing variability due to the proximity of fixed and canalized sources.

The statistical analysis of the collected data, through contaminant profiles, hierarchical clustering, and PCA, demonstrated the possibility of evaluating the contributions of peculiar industrial activities, in particular steel industry, from lichen sample pollutant concentrations. The specificity of a Mo-PCDD component supports this capability and shows that more specific markers can characterize some atmospheric

emission profiles with enhanced reliability and reduced mixing of sources in the components, as generally admitted in atmospheric source apportionment works. Thereby, source evaluation in lichens could benefit from known atmospheric markers, such as levoglucosan to discriminate biomass burning and hopanes to identify oil-related origins, as these organic compounds may also accumulate in lichens just as PAHs, PCBs, or PCDD/Fs. Furthermore, with an adequate number of observations along with well-chosen markers and a sufficient knowledge of the local emission sources, improved statistical analysis such as PMF could be considered in further works. Then, the estimation of sources contributions could take a spatial dimension, at the lichen bioaccumulation time scale integrating relatively long periods.

Acknowledgments The authors are particularly thankful to Y. Agnan for technical support. Acknowledgements are also addressed to “La Drôme Laboratoire” for detailed results and analytical protocol regarding PCDD/F analyses, Météo-France for meteorological data through the agreement N° DIRSE/REC/16/02/0, and the Vigueirat natural reserve and harbor authorities and local collectivities for authorizing sampling sites in restricted areas.

References

- Adams MD, Gottardo C (2012) Measuring lichen specimen characteristics to reduce relative local uncertainties for trace element biomonitoring. *Atmos Pollut Res* 3(3):325–330. <https://doi.org/10.5094/APR.2012.036>
- Agan Y, Séjalon-Delmas N, Claustres A, Probst A (2015) Investigation of spatial and temporal metal atmospheric deposition in France through lichen and moss bioaccumulation over one century. *Sci Total Environ* 529:285–296. <https://doi.org/10.1016/j.scitotenv.2015.05.083>
- Anderson PN, Hites RA (1996) OH radical reactions: the major removal pathway for polychlorinated biphenyls from the atmosphere. *Environ Sci Technol* 30(5):1756–1763. <https://doi.org/10.1021/es950765k>
- Atkinson R (1996) Atmospheric chemistry of PCBs, PCDDs and PCDFs (chap. 6). In: Hester RE, Harrison RM (eds) *Issues in environmental science and technology—6. Chlorinated organic micropollutants*. The Royal Society of Chemistry, Cambridge (UK), pp 53–72
- Atkinson R, Arey J (1994) Atmospheric chemistry of gas-phase polycyclic aromatic hydrocarbons: formation of atmospheric mutagens. *Environ Health Perspect* 102(Suppl 4):117–126. <https://doi.org/10.1289/ehp.94102s4117>
- Augusto S, Máguas C, Matos J, Pereira MJ, Soares A, Branquinho C (2009) Spatial modeling of PAHs in lichens for fingerprinting of multisource atmospheric pollution. *Environ Sci Technol* 43(20):7762–7769. <https://doi.org/10.1021/es901024w>
- Augusto S, Máguas C, Branquinho C (2013) Guidelines for biomonitoring persistent organic pollutants (POPs), using lichens and aquatic mosses—a review. *Environ Pollut* 180:330–338. <https://doi.org/10.1016/j.envpol.2013.05.019>
- Augusto S, Pinho P, Santos A, Botelho M, Palma-Oliveira J, Branquinho C (2015) Declining trends of PCDD/Fs in lichens over a decade in a Mediterranean area with multiple pollution sources. *Sci Total Environ* 508:95–100. <https://doi.org/10.1016/j.scitotenv.2014.11.065>

- Augusto S, Pinho P, Santos A, Botelho M, Palma-Oliveira J, Branquinho C (2016) Tracking the spatial fate of PCDD/F emissions from a cement plant by using lichens as environmental biomonitors. *Environ Sci Technol* 50(5):2434–2441. <https://doi.org/10.1021/acs.est.5b04873>
- Bajpai R, Upreti DK, Dwivedi SK, Nayaka S (2009) Lichen as quantitative biomonitors of atmospheric heavy metals in Central India. *J Atmos Chem* 63(3):235–246. <https://doi.org/10.1007/s10874-010-9166-x>
- Boampong LK, de Freitas CR, Williams D (2017) Source apportionment of air pollutants in the Greater Auckland Region of New Zealand using receptor models and elemental levels in the lichen, *Parmotrema reticulatum*. *Atmos Pollut Res* 8(1):101–113. <https://doi.org/10.1016/j.apr.2016.07.012>
- Boonpeng C, Polyiam W, Sriviboon C, Sangiamdee D, Watthana S, Nimis PL, Boonpragob K (2017) Airborne trace elements near a petrochemical industrial complex in Thailand assessed by the lichen *Parmotrema tinctorum* (Despr. ex. Nyl.) Hale. *Environ Sci Pollut Res* 24(13):12393–12404. <https://doi.org/10.1007/s11356-017-8893-9>
- Brunialti G, Frati L (2007) Biomonitoring of nine elements by the lichen *Xanthoria parietina* in Adriatic Italy: a retrospective study over a 7-year time span. *Sci Total Environ* 387(1-3):289–300. <https://doi.org/10.1016/j.scitotenv.2007.06.033>
- Christensen ER, Steinnes E, Eggen OA (2018) Anthropogenic and geogenic mass input of trace elements to moss and natural surface soil in Norway. *Sci Total Environ* 613-614:371–378. <https://doi.org/10.1016/j.scitotenv.2017.09.094>
- Daimari R, Hoque RR, Nayaka S, Upreti DK (2013) Atmospheric heavy metal accumulation in epiphytic lichens and their phorophytes in the Brahmaputra Valley. *Asian J Water Environ Pollut* 10(4):1–12
- de Mendiburu F (2017) *Agricolae*: statistical procedures for agricultural research. R package version 1.2-8. (URL: <https://CRAN.R-project.org/package=agricolae>)
- Demiray AD, Yolcubal I, Akyol NH, Cobanoglu G (2012) Biomonitoring of airborne metals using the lichen *Xanthoria parietina* in Kocaeli Province, Turkey. *Ecol Indic* 18:632–643. <https://doi.org/10.1016/j.ecolind.2012.01.024>
- Dimashki M, Lim LH, Harrison RM, Harrad S (2001) Temporal trends, temperature dependence, and relative reactivity of atmospheric polycyclic aromatic hydrocarbons. *Environ Sci Technol* 35(11):2264–2267. <https://doi.org/10.1021/es000232y>
- Domeño C, Blasco M, Sánchez C, Nerin C (2006) A fast extraction technique for extracting polycyclic aromatic hydrocarbons (PAHs) from lichens samples used as biomonitors of air pollution: dynamic sonication versus other methods. *Anal Chim Acta* 569(1-2):103–112. <https://doi.org/10.1016/j.aca.2006.03.053>
- Dominguez-Moruco N, Augusto S, Tralabal L, Pocurull E, Borrull F, Schuhmacher M, Domingo JL, Nadal M (2017) Monitoring PAHs in the petrochemical area of Tarragona County, Spain: comparing passive air samplers with lichen transplants. *Environ Sci Pollut Res* 24(13):11890–11900. <https://doi.org/10.1007/s11356-015-5612-2>
- Dron J, Chamaret P (2015) Investigating molybdenum emissions from the Lyondell Chimie France industrial site in Fos-sur-Mer. Final report, Institut Ecocitoyen pour la Connaissance des Pollutions, Fos-sur-Mer, France. (confidential)
- Dron J, Austruy A, Agnan Y, Ratier A, Chamaret P (2016) Biomonitoring with lichens in the industrialo-portuary zone of Fos-sur-Mer (France): feedback on three years of monitoring at a local collectivity scale. *Pollution Atmosphérique* 228. (URL: <http://odel.irevues.inist.fr/pollution-atmospherique/index.php?id=5392>, written in French with abstract and captions in English)
- European Commission (EC) (2011) Regulation No 1259/2011 of 2 December 2011 amending Regulation No 1881/2006 as regards maximum levels for dioxins, dioxin-like PCBs and non dioxin-like PCBs in foodstuffs. (URL: <http://data.europa.eu/eli/reg/2011/1259/oj>)
- European Environment Agency (EEA) (2016) Air quality in Europe—2016 report, Copenhagen, Denmark (URL: <http://www.eea.europa.eu/publications/air-quality-in-europe-2016>)
- Hissler C, Stille P, Krein A, Geagea ML, Perrone T, Probst J-L, Hoffmann L (2008) Identifying the origins of local atmospheric deposition in the steel industry basin of Luxembourg using the chemical and isotopic composition of the lichen *Xanthoria parietina*. *Sci Total Environ* 405(1-3):338–344. <https://doi.org/10.1016/j.scitotenv.2008.05.029>
- International Agency for Research on Cancer (IARC) (2013) In: Straif K, Cohen A, Samet J (eds) *Air pollution and cancer*, IARC Scientific Publication 161: IARC, Lyon, France
- Kodnik D, Carniel FC, Licen S, Tolloi A, Barbieri P, Tretiac M (2015) Seasonal variations of PAHs content and distribution patterns in a mixed land use area: a case study in NE Italy with the transplanted lichen *Pseudevernia furfuracea*. *Atmos Environ* 113:255–263. <https://doi.org/10.1016/j.atmosenv.2015.04.067>
- Liu H-J, Zhao L-C, Fang S-B, Liu S-W, J-S H, Wang L, Liu X-D, Q-F W (2016) Use of the lichen *Xanthoria mandshurica* in monitoring atmospheric elemental deposition in the Taihang Mountains, Hebei, China. *Sci Rep* 6(1):23456. <https://doi.org/10.1038/srep23456>
- Lough GC, Schauer JJ, Park J-S, Shafer MM, DeMinter JT, Weinstein JP (2005) Emissions of metals associated with motor vehicle roadways. *Environ Sci Technol* 39(3):826–836. <https://doi.org/10.1021/es048715f>
- Murtagh F, Legendre P (2014) Ward’s hierarchical agglomerative clustering method: which algorithms implement Ward’s criterion? *J Classif* 31(3):274–295. <https://doi.org/10.1007/s00357-014-9161-z>
- Nimis PL, Scheidegger C, Wolseley PA (eds) (2002) *Monitoring with lichens—monitoring lichens*, NATO Science Series - Kluwer Academic Publishers, Dordrecht
- Occelli F, Cuny M-A, Devred I, Deram A, Quarré S, Cuny D (2013) Étude de l’imprégnation de l’environnement de trois bassins de vie de la région Nord-Pas-de-Calais par les éléments traces métalliques. *Pollution Atmosphérique* 220. (URL: <http://odel.irevues.inist.fr/pollution-atmospherique/index.php?id=2497>, written in French with abstract and captions in English)
- Occelli F, Bavdek R, Deram A, Hellequin A-P, Cuny M-A, Zwarterook I, Cuny D (2016) Using lichen biomonitoring to assess environmental justice at a neighborhood level in an industrial area of Northern France. *Ecol Indic* 60:781–788. <https://doi.org/10.1016/j.ecolind.2015.08.026>
- Park H, Lee S-H, Kim M, Kim J-H, Lim HS (2010) Polychlorinated biphenyl congeners in soils and lichens from King George Island, South Shetland Islands, Antarctica. *Antarct Sci* 22(01):31–38. <https://doi.org/10.1017/S0954102009990472>
- Pernigotti D, Belis CA, Spanò L (2016) SPECIEUROPE: the European data base for PM source profiles. *Atmos Pollut Res* 7(2):307–314. <https://doi.org/10.1016/j.apr.2015.10.007>
- Protano C, Owczarek M, Fantozzi L, Guidotti M, Vitali M (2015) Transplanted lichen *Pseudevernia furfuracea* as a multi-tracer monitoring tool near a solid waste incinerator in Italy: assessment of airborne incinerator-related pollutants. *Bull Environ Contam Toxicol* 95(5):644–653. <https://doi.org/10.1007/s00128-015-1614-5>
- R Core Team (2016) R: A language and environment for statistical computing. R Foundation for Statistical Computing: Vienna, Austria. (URL: <https://www.R-project.org/>)
- Reimann C, Filzmoser P, Garrett R, Dutter R (eds) (2008) *Statistical data analysis explained—applied environmental statistics with R*. John Wiley and Sons Ltd., West Sussex. <https://doi.org/10.1002/9780470987605>
- Sarrazin L, Diana C, Wafu E, Pichard-Lagadec V, Schembri T, Monod J (2006) Determination of polycyclic aromatic hydrocarbons (PAHs)

- in marine, brackish, and river sediments by HPLC, following ultrasonic extraction. *J Liq Chromatogr Relat Technol* 29(1):69–85. <https://doi.org/10.1080/10826070500362987>
- Sternbeck J, Sjödin A, Andréasson K (2002) Metal emissions from road traffic and the influence of resuspension—results from two tunnel studies. *Atmos Environ* 36(30):4735–4744. [https://doi.org/10.1016/S1352-2310\(02\)00561-7](https://doi.org/10.1016/S1352-2310(02)00561-7)
- Stockholm Convention on Persistent Organic Pollutants (2001) United Nations, Stockholm, Sweden. (URL: <http://chm.pops.int/Default.aspx>)
- Sylvestre A (2016) Characterization of industrial aerosols and quantification of its contribution in atmospheric PM_{2.5}. Ph.D. Dissertation, Aix-Marseille University, Marseille, France [in French with large English inclusions]
- Sylvestre A, Mizzi A, Mathiot S, Masson F, Jaffrezzo J-L, Dron J, Mesbah B, Wortham H, Marchand N (2017) Comprehensive chemical characterization of industrial PM_{2.5}: steel plant activities. *Atmos Environ* 152:180–190. <https://doi.org/10.1016/j.atmosenv.2016.12.032>
- Van den Berg M, Birnbaum LS, Denison M, De Vito M, Farland W, Feeley M, Fiedler H, Hakansson H, Hanberg A, Haws L, Rose M, Safe S, Schrenk D, Tohyama C, Tritscher A, Tuomisto J, Tysklind M, Walker N, Peterson RE (2006) The 2005 World Health Organization reevaluation of human and mammalian toxic equivalency factors for dioxins and dioxin-like compounds. *Toxicol Sci* 93(2):223–241. <https://doi.org/10.1093/toxsci/kfl055>
- Van der Wat PF, Forbes PBC (2015) Lichens as biomonitors for organic air pollutants. *Trends Anal Chem* 64:165–172
- Veschambre S, Moldovan M, Amouroux D, Santamaria Ulecia JM, Benech B, Etchelecou A, Losno R, Donard, OF-X, Pinel-Raffaitin P (2008) Import of atmospheric trace metal elements in the Aspe valley and Somport tunnel (Pyrénées Atlantiques, France): level of contamination and evaluation of emission sources. *Pollution Atmosphérique* 198–199 (URL: <http://odel.irevues.inist.fr/pollution-atmospherique/index.php?id=1342>, written in French with abstract and captions in English)
- Viana M, Kuhlbusch T, Querol X, Alastuey A, Harrison R, Hopke P, Winiwarter W, Vallius M, Szidat S, Prévôt A, Hueglin C, Bloemen H, Wahlin P, Vecchi R, Miranda A, Kasper-Giebl A, Maenhaut W, Hitzenberger R (2008) Source apportionment of particulate matter in Europe: a review of methods and results. *J Aerosol Sci* 39:827–849
- Wafu E, Sarrazin L, Diana C, Schembri T, Lagadec V, Monod J-L (2006) Polychlorinated biphenyls and DDT residues distribution in sediments of Cortiou (Marseille, France). *Mar Pollut Bull* 52(1):104–107. <https://doi.org/10.1016/j.marpolbul.2005.09.041>
- Zhu N, Schramm K-W, Wang T, Henkelmann B, Fu J, Gao Y, Wang Y, Jiang G (2015) Lichen, moss and soil in resolving the occurrence of semi-volatile organic compounds on the southeastern Tibetan Plateau, China. *Sci Total Environ* 518–519:328–336

Characterization of atmospheric emission sources in lichen from metal and organic contaminant patterns

Aude Ratier, Julien Dron, Gautier Revenko, Annabelle Austruy, Charles-Enzo Dauphin, Florence Chaspoul, Emmanuel Wafo

SUPPLEMENTARY MATERIAL

FIGURE S1. Photography of sampling epiphytic *Xanthoria parietina* thalli (photo credits: J.Dron/IECP).

SUPPLEMENTARY INFORMATION S1. Chemical analyses quality control.

TABLE S1. Analytical performances and quality tests for metal and metalloid analyses.

TABLE S2. Analytical performances and quality tests for individual PAH congeners.

TABLE S3. Analytical performances and quality tests for individual PCB congeners.

FIGURE S2. Spatial distributions of metal elements Al, Fe, V, Cr, Mo, Ni, Cu, Sb.

FIGURE S3. Distribution of metal and metalloid standardized (z-scores) levels according to the sampling stations categories.

TABLE S4. Mean concentrations and standard deviations for PAH congeners measured in *X. parietina* samples according to site categories

TABLE S5. Mean concentrations and standard deviations for PCDD/F congeners measured in *X. parietina* samples according to site categories

TABLE S6. Mean concentrations and standard deviations for PCB congeners measured in *X. parietina* samples according to site categories

FIGURE S1

Photography of sampling epiphytic *Xanthoria parietina* thalli (photo credits: J.Dron/IECP).



SUPPLEMENTARY INFORMATION S1. Chemicals and analyses quality control.

Chemicals and materials

Water used for all manipulations was always ultrapure (resistivity 18.2 M Ω .cm). The glassware and all laboratory and sampling materials were cleaned with diluted hydrochloric acid and acetone (or detergent TFD4 dec FT30), rinsed several times after each step with ultrapure water, and oven dried at 80 °C (sampling materials) or 200 °C (analytical materials). The analytical materials were finally rinsed twice with the corresponding solvent before use.

Metals mineralization acids were Superpure for trace analysis grade (Carlo Erba) HCl 34-37 % and HNO₃ (67-69 %). The standards were prepared from the multi-element solution for ICP/MS (certified reference materials) purchased from Sigma-Aldrich.

The n-hexane used for the PCB extraction was Pestipur grade (Carlo Erba) and the sulfuric acid RPE 96 % grade (Carlo Erba). The PCB standards were realized from a PCB Congener Mix (each at 10 $\mu\text{g.L}^{-1}$ in isooctane, Accustandard).

Methanol and acetone used in the PAH extraction steps were RPE for analysis and RS for HPLC grades, respectively (Carlo Erba). The PAH standard solution (PAH solution mix, Accustandard) contained each of the 16 congeners from the USEPA priority list at a 0.2 mg.L^{-1} concentration in CH₂Cl₂/MeOH (50:50, v:v).

Quality controls methods

Metal elements ICP-MS analysis was controlled by determining the lichen and ray-grass certified materials IAEA-336 and ERM CD-281 (Table S1). As no lichen or similar certified material is available commercially for PAH and PCB, a marine clam certified sample (IAEA 451) with comparable concentration values was chosen (Table S2 and S3, respectively).

For a more robust validation of PAH and PCB analyses, additional quality tests were realized by determining the analytical recoveries using a test lichen sample collected near station #6 and spiked with standard solutions. The test sample was Soxhlet extracted during 16 h at 45 °C and dried at 105 °C to remove initially present PAHs and PCBs, and finally stored for 24 h in a dessicator. About 500 mg of test lichen was then spiked with a standard solution. In the case of PAHs, the Accustandard PAH solution mix (Interchim) was added at the concentrations 6.25 and 50 $\mu\text{g.L}^{-1}$ which correspond to “mid” and “high” levels in the calibration curves (analytical range is 0.31 - 50 $\mu\text{g.L}^{-1}$, linearity > 0.999). For PCBs, the spiking levels were 1.56, 12.5 and 50 $\mu\text{g.L}^{-1}$ which are the “low”, “mid” and “high” levels in the calibration range (1.56-50 $\mu\text{g.L}^{-1}$, linearity > 0.994).

Polychlorodibenzodioxins and furans (PCDD/F)

PCDD/F analyses were realized in the Drôme departmental laboratory (La Drôme Laboratoires, Valence, France). The laboratory is granted with the ISO 17025:2005 certification, attributed by the French Committee for Accreditation (Cofrac), covering foodstuffs, solids, environment and air quality among other. This implies that regular quality controls including recoveries and determination of standard deviations and detection limits fulfill the requirements of analytical quality requested by the ISO and Cofrac certifications.

Recoveries were determined by spiked ¹³C-labeled standards and corrections were applied to each sample individually for each corresponding PCDD/F.

Table S1. Analytical performances and quality tests for metal and metalloid analyses. RSD and detection limits are based on regular daily or weekly calculations and the later depend on samples quantities.

congeners	RSD %	Lichen IAEA 336 measured (recommended) mg.kg ⁻¹	Rye grass ERM CD281 measured (certified) mg.kg ⁻¹	Detection limits mg.kg ⁻¹
Al	10	555 (680*)		0.1
V	5	1.51 (1.47*)		0.1
Cr	5	1.25 (1.06*)	24.6 (24.8 ± 1.3)	0.1
Mn	5	63 (63 ± 7)	77 (82 ± 4)	0.1
Fe	10	414 (430 ± 50)	205 (180*)	0.1
Co	5	0.25 (0.29 ± 0.05)		0.1
Ni	5		15.1 (15.2 ± 0.6)	0.1
Cu	5	3.59 (3.60 ± 0.04)	10.2 (10.2 ± 0.5)	0.1
Zn	10	31.0 (30.4 ± 3.4)	30.7 (30.5 ± 1.1)	0.1
As	5	0.66 (0.63 ± 0.08)	0.039 (0.042 ± 0.010)	0.05
Mo	5		2.51 (2.22 ± 0.12)	0.1
Ag	5			0.1
Cd	5	0.10 (0.12*)	0.118 (0.120 ± 0.007)	0.05
Sn	5		0.070 (0.062 ± 0.011)	0.05
Sb	5	nd (0.07 ± 0.01)	0.040 (0.042 ± 0.007)	0.05
Hg	5	0.19 (0.20 ± 0.04)	nd (0.016 ± 0.002)	0.1
Tl	5			0.1
Pb	5	4.69 (4.90*)	1.53 (1.67 ± 0.11)	0.1

* Information values

Table S2. Analytical performances and quality tests for individual PAH congeners. Detection limits are estimated from weekly determinations and depend on sample quantities.

congeners	Mean RSD % (duplicates of N=27 field samples)	Recoveries % (spiked test sample) mid (N=3) and high range (N=3)		Clam IAEA 451 measured (certified) $\mu\text{g}\cdot\text{kg}^{-1}$		Detection limits $\mu\text{g}\cdot\text{kg}^{-1}$
Nap	8.8	80.0	80.7	14.9	(14.8 \pm 1.2)	1
Acy	4.8	82.9	86.0	2.2	(2.2*)	1
Ace	3.2	72.8	80.5	2.2	(2.0*)	1
Flu	7.6	79.1	92.6	1.9	(2.6*)	1
Phe	3.8	86.7	89.5	17.1	(15.8 \pm 5.6)	1
Ant	13.1	74.7	83.4	6.1	(5.1*)	1
FIA	11.9	85.1	80.1	51.7	(49.3 \pm 3.2)	1
Pyr	5.3	77.0	87.8	37.9	(40.0 \pm 4.6)	1
BaA	6.1	86.0	86.7	19.4	(19.2 \pm 1.3)	1
Chr	7.7	86.0	90.2	27.6	(26.9 \pm 2.0)	1
BbF	6.0	96.3	88.8	35.1	(35.8 \pm 6.2)	1
BkF	4.8	75.1	93.2	12.7	(14.7 \pm 3.2)	1
BaP	3.0	84.3	98.4	18.9	(18.2 \pm 2.4)	1
BPe	9.6	84.3	89.5	22.5	(19.5 \pm 2.4)	1
DBA	5.9	99.3	91.0	16.1	(5.3 \pm 1.4)	1
IPy	16.2	99.4	71.1	23.0	(23.8*)	1

* Recommended or information values

Table S3. Analytical performances and quality tests for individual PCB congeners. Detection limits are estimated among weekly determinations and depend on sample quantities. Indicator PCB are marked as (i).

congeners	Mean RSD % (duplicates of N=13 field samples)	Recoveries % (spiked test sample)			Clam IAEA 451 measured (certified) $\mu\text{g.kg}^{-1}$		Detection limits $\mu\text{g.kg}^{-1}$
		low (N=1)	mid (N=2)	and high range (N=10)			
28 (i)	28.9	85.3	91.3	91.0	0.50	(0.85 \pm 0.09)	0.01
52 (i)	16.6	95.7	99.5	92.7	0.53	(0.82 \pm 0.04)	0.01
101 (i)	15.1	123.8	107.8	93.3	1.25	(1.74 \pm 0.14)	0.01
105	66.2	69.9	74.2	91.5	0.55	(0.49 \pm 0.12)	0.01
118	17.8	118.6	106.5	89.1	0.83	(1.01 \pm 0.08)	0.01
123	26.8	not determined			not determined		0.01
138 (i)	14.9	93.6	86.2	91.8	5.51	(5.30 \pm 0.58)	0.01
153 (i)	12.0	96.2	108.7	92.6	9.36	(8.59 \pm 0.78)	0.01
156	nd	70.4	94.7	95.2	0.98	(0.56*)	0.01
180 (i)	28.5	101.7	94.9	92.0	6.60	(6.56 \pm 1.20)	0.01

* Information value

FIGURE S2

Metal elements spatial distributions (Al, Fe, expressed in $\text{g}\cdot\text{kg}^{-1}$ dw ; V, Cr, in $\text{mg}\cdot\text{kg}^{-1}$ dw).

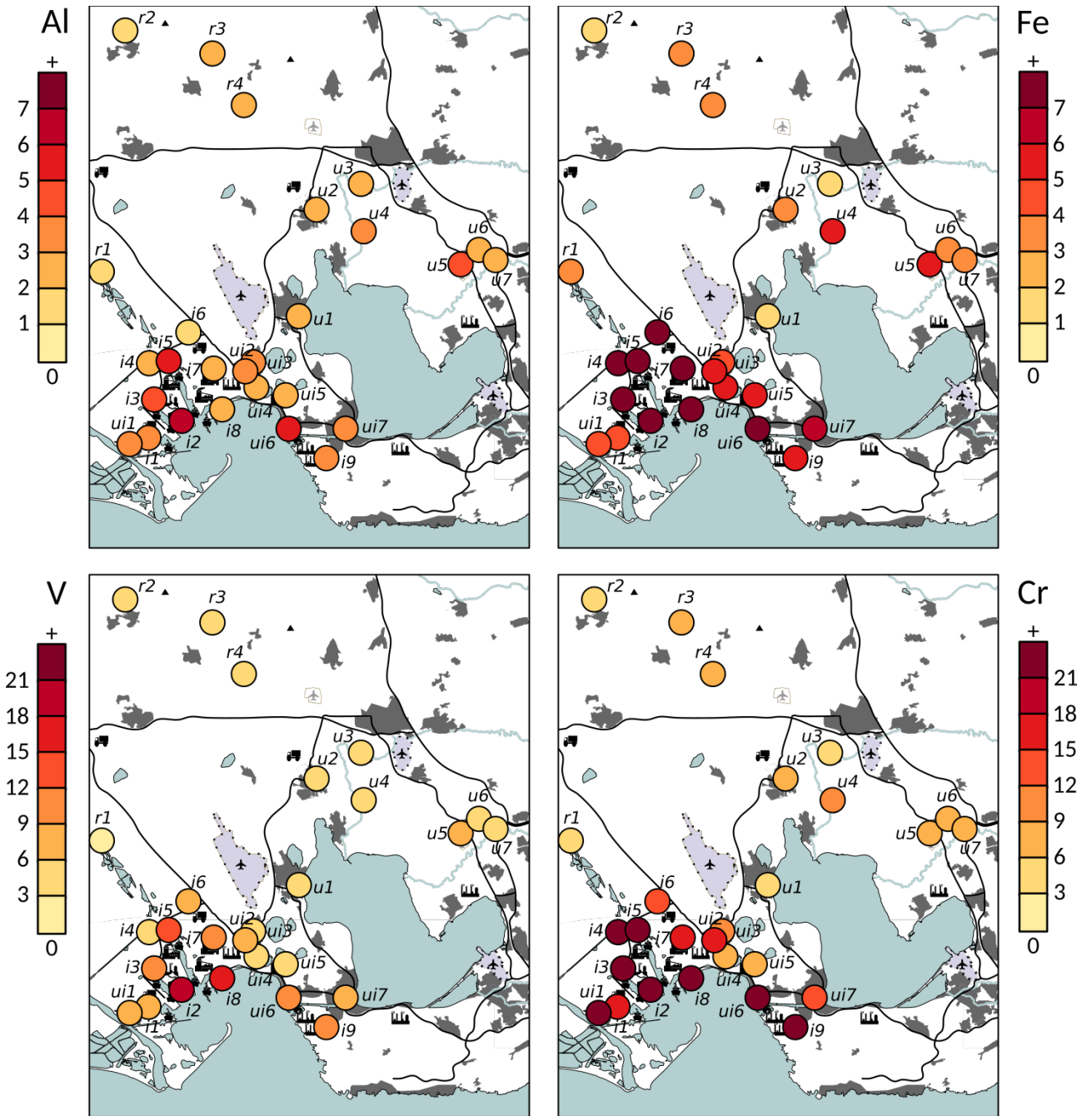


FIGURE S2 (continued)

Metal elements spatial distributions (Mo, Ni, Cu, Sb, in $\text{mg}\cdot\text{kg}^{-1}$ dw).

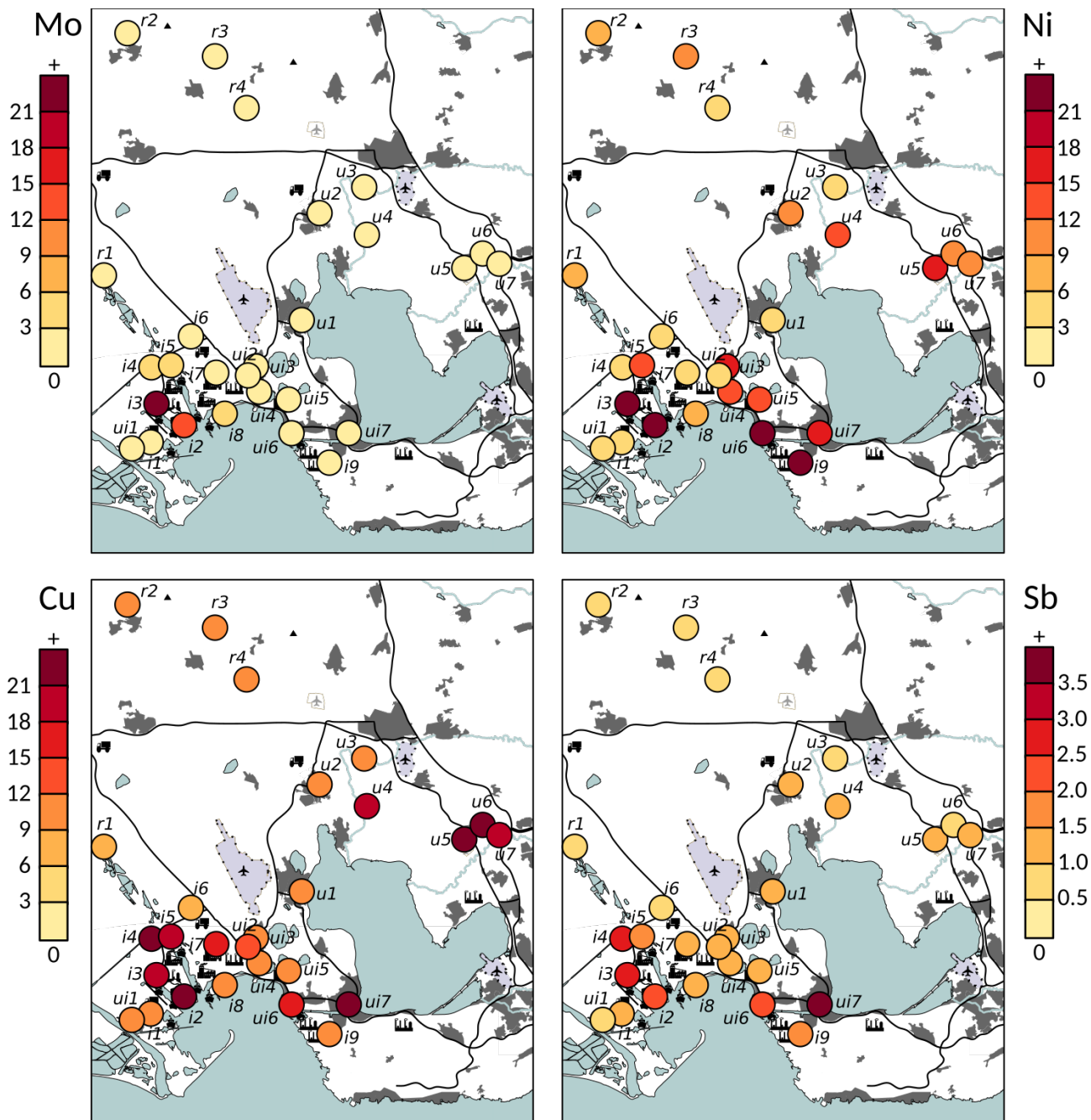


FIGURE S3

Distribution of metal and metalloid standardized (z-scores) levels according to the sampling stations categories.

Boxplots represent the median values (white or black lines), 1st and 3rd quartiles (box limits) and most extreme data or 1.5-times the interquartile range if outliers (whiskers).

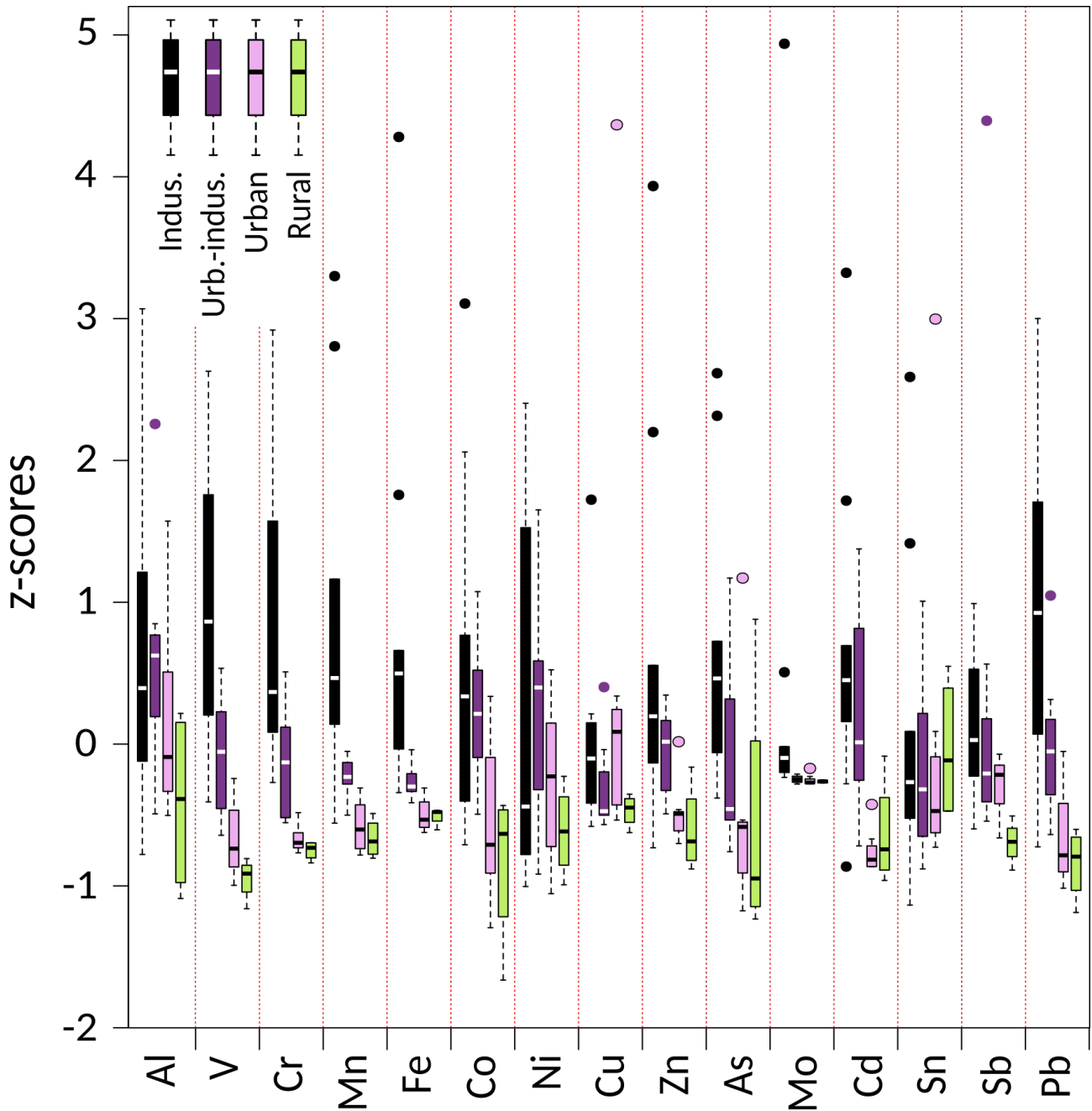


TABLE S4. Mean concentrations and standard deviations for PAH congeners ($\mu\text{g.kg}^{-1}$ dw) measured in *X. parietina* samples according to site categories (N = 9 ; N = 7 ; N = 7 ; N = 4 in industrial, urban-industrial, urban, rural categories, respectively).

congener	Industrial	Urban-ind.	Urban	Rural
Nap	96.4 \pm 75.0	37.0 \pm 21.9	41.6 \pm 7.8	32.2 \pm 16.3
Acy	130 \pm 106	183 \pm 60	154 \pm 69	137 \pm 47
Ace	198 \pm 163	106 \pm 47	60.3 \pm 43.5	63.9 \pm 22.4
Flu	43.2 \pm 13.4	30.6 \pm 13.9	26.9 \pm 9.5	30.7 \pm 7.1
Phe	245 \pm 87	251 \pm 55	234 \pm 84	139 \pm 26
Ant	16.6 \pm 10.3	9.84 \pm 1.63	9.11 \pm 4.12	11.2 \pm 1.9
FIA	13.4 \pm 3.3	9.96 \pm 1.75	11.4 \pm 5.4	7.84 \pm 1.09
Pyr	58.4 \pm 21.0	52.6 \pm 16.7	47.5 \pm 15.3	35.5 \pm 7.6
BaA	31.6 \pm 14.6	37.4 \pm 15.7	46.3 \pm 8.2	60.2 \pm 15.3
Chr	20.0 \pm 9.7	18.4 \pm 17.4	10.9 \pm 6.2	15.9 \pm 3.5
BbF	12.0 \pm 5.5	10.6 \pm 2.6	7.88 \pm 0.70	8.08 \pm 0.24
BkF	6.98 \pm 1.29	6.75 \pm 1.03	5.45 \pm 0.22	5.78 \pm 0.15
BaP	12.2 \pm 3.3	13.6 \pm 4.7	7.95 \pm 2.42	10.1 \pm 3.6
BPe	12.4 \pm 4.7	11.6 \pm 2.4	9.66 \pm 0.77	9.96 \pm 1.21
DBA	6.58 \pm 3.63	5.42 \pm 2.18	2.15 \pm 1.40	1.68 \pm 0.58
IPy	2.27 \pm 1.84	0.57 \pm 0.23	0.47 \pm 0.47	0.18 \pm 0.02

TABLE S5. Mean concentrations and standard deviations for PCDD/F congeners (ng.kg⁻¹ dw) measured in *X. parietina* samples according to site categories (N = 9 ; N = 7 ; N = 4 ; N = 4 in industrial, urban-industrial, urban, rural categories, respectively).

congener	Industrial	Urban-ind.	Urban	Rural
2,3,7,8-TeCDD	0.16 ± 0.05	0.18 ± 0.07	0.14 ± 0.06	0.17 ± 0.04
1,2,3,7,8-PeCDD	1.13 ± 0.83	0.41 ± 0.25	0.80 ± 0.33	0.61 ± 0.34
1,2,3,4,7,8-HeCDD	0.76 ± 0.49	0.44 ± 0.06	0.39 ± 0.14	0.43 ± 0.20
1,2,3,6,7,8-HeCDD	1.82 ± 1.40	0.88 ± 0.29	1.17 ± 0.50	1.13 ± 0.23
1,2,3,7,8,9-HeCDD	1.05 ± 0.72	0.62 ± 0.11	0.86 ± 0.42	0.73 ± 0.22
1,2,3,4,6,7,8-HpCDD	8.65 ± 5.16	7.18 ± 2.29	7.80 ± 1.73	4.91 ± 0.65
OCDD	37.8 ± 35.5	37.0 ± 21.5	47.1 ± 39.3	14.5 ± 3.5
2,3,7,8-TeCDF	2.04 ± 1.06	1.51 ± 0.39	1.26 ± 0.26	1.07 ± 0.35
1,2,3,7,8-PeCDF	3.58 ± 5.69	1.13 ± 0.23	1.20 ± 0.30	1.21 ± 0.16
2,3,4,7,8-PeCDF	2.48 ± 1.48	1.30 ± 0.31	1.76 ± 0.53	1.30 ± 0.52
1,2,3,4,7,8-HeCDF	3.37 ± 4.22	1.05 ± 0.30	0.98 ± 0.35	0.97 ± 0.26
1,2,3,6,7,8-HeCDF	3.13 ± 3.78	0.96 ± 0.24	0.84 ± 0.35	0.89 ± 0.24
2,3,4,6,7,8-HeCDF	0.32 ± 0.42	0.13 ± 0.05	0.17 ± 0.10	0.19 ± 0.06
1,2,3,7,8,9-HeCDF	1.95 ± 1.83	0.73 ± 0.12	0.84 ± 0.34	0.71 ± 0.16
1,2,3,4,6,7,8-HpCDF	11.4 ± 13.4	3.59 ± 1.38	2.77 ± 0.56	2.05 ± 0.19
1,2,3,4,7,8,9-HpCDF	1.62 ± 2.35	0.30 ± 0.15	0.35 ± 0.22	0.31 ± 0.29
OCDF	34.5 ± 68.4	6.65 ± 5.34	7.21 ± 9.34	2.81 ± 0.85

TABLE S6. Mean concentrations and standard deviations for PCB congeners ($\mu\text{g.kg}^{-1}$ dw) measured in *X. parietina* samples according to site categories (N = 3 ; N = 2 ; N = 6 ; N = 2 in industrial, urban-industrial, urban, rural categories, respectively).

congener		Industrial	Urban-ind.	Urban	Rural
28	i	2.15 \pm 1.46	1.38 \pm 1.12	1.81 \pm 1.30	1.79 \pm 1.19
52	i	1.16 \pm 0.20	0.97 \pm 0.04	1.47 \pm 0.26	1.21 \pm 0.12
101	i	1.45 \pm 0.39	1.33 \pm 0.42	2.83 \pm 0.94	1.60 \pm 0.02
105	DL	0.04 \pm 0.02	0.05 \pm 0.01	0.18 \pm 0.18	0.08 \pm 0.08
118	DL	1.21 \pm 0.22	0.88 \pm 0.26	2.00 \pm 0.52	1.51 \pm 0.05
123	DL	0.62 \pm 0.15	0.41 \pm 0.02	0.68 \pm 0.36	0.33 \pm 0.11
138	i	1.55 \pm 0.41	1.45 \pm 0.13	1.88 \pm 0.79	1.15 \pm 0.03
153	i	1.39 \pm 0.11	1.21 \pm 0.12	1.32 \pm 0.63	0.72 \pm 0.00
180	i	0.54 \pm 0.15	0.61 \pm 0.17	0.18 \pm 0.12	0.06 \pm 0.02